JVI Journals.ASM.org

# Henipavirus Pathogenesis in Human Respiratory Epithelial Cells

**Olivier Escaffre,[a] Viktoriya Borisevich,[a] J. Russ Carmical,[c] Deborah Prusak,[c] Joseph Prescott,[d] Heinz Feldmann,[d] Barry Rockx[a,b]**

Departments of Pathology,[a] Microbiology & Immunology,[b] and Biochemistry & Molecular Biology,[c] University of Texas Medical Branch, Galveston, Texas, USA; Laboratory of Virology, Division of Intramural Research, NIAID, NIH, Rocky Mountain Laboratories, Hamilton, Montana, USA[d]

**Hendra virus (HeV) and Nipah virus (NiV) are deadly zoonotic viruses for which no vaccines or therapeutics are licensed for human use. Henipavirus infection causes severe respiratory illness and encephalitis. Although the exact route of transmission in human is unknown, epidemiological studies and *in vivo* studies suggest that the respiratory tract is important for virus replication. However, the target cells in the respiratory tract are unknown, as are the mechanisms by which henipaviruses can cause disease. In this study, we characterized henipavirus pathogenesis using primary cells derived from the human respiratory tract. The growth kinetics of NiV-Malaysia, NiV-Bangladesh, and HeV were determined in bronchial/tracheal epithelial cells (NHBE) and small airway epithelial cells (SAEC). In addition, host responses to infection were assessed by gene expression analysis and immunoassays. Viruses replicated efficiently in both cell types and induced large syncytia. The host response to henipavirus infection in NHBE and SAEC highlighted a difference in the inflammatory response between HeV and NiV strains as well as intrinsic differences in the ability to mount an inflammatory response between NHBE and SAEC. These responses were highest during HeV infection in SAEC, as characterized by the levels of key cytokines (interleukin 6 [IL-6], IL-8, IL-1α, monocyte chemoattractant protein 1 [MCP-1], and colony-stimulating factors) responsible for immune cell recruitment. Finally, we identified virus strain-dependent variability in type I interferon antagonism in NHBE and SAEC: NiV-Malaysia counteracted this pathway more efficiently than NiV-Bangladesh and HeV. These results provide crucial new information in the understanding of henipavirus pathogenesis in the human respiratory tract at an early stage of infection.**

Nipah (NiV) and Hendra virus (HeV) are emerging zoonotic pathogens of the family *Paramyxoviridae* and are classified in the genus *Henipavirus* (1). NiV and HeV both cause severe and often fatal respiratory disease and/or encephalitis in animals and humans. HeV was first isolated during an outbreak of respiratory and neurologic disease in horses and humans in Australia in 1994 (2–5). To date, a total of 5 outbreaks of HeV involving human cases have been reported in Australia, and 7 human cases with a case fatality rate of 57% have been identified (6). The first human cases of NiV infection were identified during an outbreak of severe febrile encephalitis in Malaysia and Singapore in 1998-1999 (7, 8). Several other outbreaks have occurred thereafter in Bangladesh and India almost yearly since 2001 (6, 9, 10), with the last outbreak reported in Bangladesh in 2012 (11). NiV strains from Malaysia (M) and Bangladesh (B) are genetically distinct based on phylogenic analyses using amino acid sequences (6, 12). To date, NiV has been responsible for more than 500 human cases, with mortality rates ranging from 40% (in Malaysia) (13) to 100% (in Bangladesh and India) (6, 11, 14). The natural hosts of henipaviruses are fruit bats (*Pteropus* species) (15–17), and transmission of these viruses from bats to humans may be direct or via an intermediate host like horses or pigs for HeV and NiV transmission, respectively (2, 15, 18–23). Interestingly, respiratory symptoms such as cough and difficulty breathing were reported for about 70% of NiV-B-infected and less than 30% of NiV-M-infected patients (24). In addition, in recent outbreaks, a high incidence of person-to-person transmission has been reported in Bangladesh and India (9, 25, 26) as opposed to the outbreaks of NiV in Malaysia and HeV in Australia, suggesting differences in host-virus interactions between genetically distinct henipaviruses.

The main target cells during the late stage of henipavirus infection in humans are endothelial cells of blood vessels, resulting in vasculitis, vasculitis-induced thrombosis, and vascular microinfarction in the central nervous system (CNS) but also in other organs such as the lungs, spleen, and kidneys (27–29). The infection also reaches the CNS parenchymal cells, which all together play an important role in the pathogenicity of henipaviruses (27, 30).

Although the exact route of infection in humans is unknown, previous studies in several laboratory animal models reported an efficient infection through intranasal challenge (31–35), suggesting that the respiratory tract is one of the first targets of virus replication. In addition, both NiV and HeV have been isolated from oropharyngeal and respiratory secretions from humans and animals (36–38), which emphasizes the importance of the respiratory tract in virus replication and potential transmission. In hamsters, NiV infection of the respiratory tract is initiated in the trachea and progresses down the respiratory tract, infecting the bronchial epithelium and finally causing severe hemorrhagic pneumonia, including the characteristic syncytium formation in the pulmonary endothelium. In contrast, HeV infection is initiated primarily in the small airways of the lungs and not in the trachea or bronchi (34). In humans, henipavirus infection is characterized by influenza-like illness, which can progress to pneumonia (8, 13, 23, 39, 40) or acute respiratory distress syndrome (ARDS) as characterized in some cases of NiV-B infection (10).

**Received** 19 September 2012 **Accepted** 24 December 2012
**Published ahead of print** 9 January 2013
Address correspondence to Barry Rockx, barockx@UTMB.EDU.

doi:10.1128/JVI.02576-12

Interestingly, while limited data are available on the histopathology of the lungs of henipavirus cases, changes in the respiratory tract in NiV-M-infected patients include hemorrhage, necrosis, and inflammation in the epithelium of the small airways but not in the bronchi (29), similar to observations in hamsters (34) and nonhuman primates (33). Finally, lesions and inflammation were reported to occur in the small airways of HeV-infected patients (23, 28, 40); no information is available about the histopathological changes in the respiratory tract of NiV-B-infected patients. The specific sites of henipavirus infection in the human respiratory tract are still unknown, as is the mechanism by which these viruses can cause disease.

We hypothesize that the human immune response to henipavirus infection at an early step of infection can determine the clinical outcome, explain how the virus can disseminate throughout the host, and affect person-to-person transmission. To gain further insight into the early steps of infection, we conducted the first characterization of NiV and HeV infection of the human respiratory tract using primary human epithelial cells derived from the bronchi (bronchial/tracheal epithelial cells [NHBE]) and the small airways (small airway epithelial cells [SAEC]). Our results showed that the replication kinetics of genetically distinct NiV and HeV strains are efficient in both cell types and result in a differential innate immune response depending on the virus strain and the cell origin. Finally, we demonstrate a virus strain-dependent variability in type I interferon (IFN) signaling that seems independent of the origin of cells from the human respiratory tract.

## MATERIALS AND METHODS

**Viruses and cells.** NiV-Malaysia (NiV-M), NiV-Bangladesh (NiV-B), and HeV were kindly provided by the Special Pathogens Branch of the Centers for Disease Control and Prevention (Atlanta, GA). The viruses were propagated on Vero cells (CCL-81; ATCC) in Dulbecco's modified Eagle's medium with 400 mM L-glutamine, 4,500 mg/liter of glucose, and sodium pyruvate (Thermo Scientific, Logan, UT) and supplemented with 10% fetal bovine serum, 100 U/ml of penicillin, and 0.1 mg of streptomycin (Sigma-Aldrich, St. Louis, MO) at 37°C and 5% $CO_2$. Cells were seeded in 96-well plates for virus titration.

NHBE derived from the bronchial tube and normal SAEC derived from the distal airspace were obtained with the Clonetics Bronchial/Tracheal Epithelial Cell System and the Clonetics Normal Human Small Airway Epithelial Cell System (Clonetics, San Diego, CA), respectively. Monolayers of undifferentiated NHBE and SAEC were cultured in 150-$cm^2$ flasks for 8 days (37°C and 5% $CO_2$) with a bronchial epithelial cell basal medium supplied with growth factors in the BEGM BulletKit and with an SAEC basal medium supplied with growth factors in the SAGM BulletKit, respectively. All NHBE and SAEC infections were performed at a multiplicity of infection (MOI) of 5 for 1 h to ensure synchronous infection. Cells were then rinsed three times with 1× phosphate-buffered saline (PBS), and appropriate medium was added. NHBE and SAEC were seeded in 6-well plates at $1 \times 10^6$ cells/well (each condition performed in triplicate) the day prior to infection for virus replication, gene expression, and cytokine and chemokine quantification. NHBE and SAEC were seeded in 12-well plates at $3.5 \times 10^5$ cells/well (each condition performed in triplicate) the day prior to infection for the quantification of Stat1 and phospho-Stat1 (p-Stat1) by Western blotting.

Viruses were titrated on Vero cells in 96-well plates using 10-fold virus dilutions in triplicate. Virus titer was expressed as median 50% tissue culture infective dose ($TCID_{50}$)/ml using the method of Reed and Muench (41). All work with live viruses was performed in Galveston National Laboratory Level 4 (biosafety level 4 [BSL4]) at the University of Texas Medical Branch.

**Gene expression analysis.** Total cellular RNA from NHBE and SAEC was extracted at 24 h postinfection (p.i.) in triplicate using TRIzol reagent (Invitrogen, Carlsbad, CA) according to the manufacturer's recommendations. RNA was quantified using a NanoDrop ND-1000 (NanoDrop Technologies, Wilmington, DE) and RNA integrity assessed by visualization of 18S and 28S RNA bands using an Agilent BioAnalyzer 2100 (Agilent Technologies, Santa Clara, CA). Total RNA extracted from the samples was processed using the RNA labeling protocol described by Ambion (MessageAmp aRNA kit instruction manual) and hybridized to Affymetrix Gene Chips (HGU133 Plus 2.0 arrays, total genome). Data quality was assessed by applying the quality matrix generated by the Affymetrix GeneChip Command Console (AGCC) software. The resulting data were analyzed with Partek Genomics Suite (Partek, St. Louis, MO). Principal-component analysis as a quality assurance measure was performed. The raw data were normalized through robust multichip averaging upon import to Partek Genomics Suite. An analysis of variance (ANOVA) was carried out and a false discovery rate (FDR) applied to reduce the occurrence of false positives. The data set was filtered for a $P$ value of 0.05 and a cutoff of ≥2.00, resulting in the final list of differentially expressed genes. Ingenuity Pathway Analysis (IPA) software and iReport (Ingenuity Systems, Redwood City, CA) were then used to analyze and interpret data. The analyses of the most significant biological functional groups and canonical pathways affected per condition were performed using an uncorrected $P$ value calculation method [right-tailed Fisher exact method, $P < 0.05$ or $-\log(P \text{ value}) > 1.3$]. A ratio (r) accounting for the number of overlapping genes from a particular pathway was also introduced to help in the analyses of filtered data.

**Real-time SYBR green qPCR assay design.** Real-time quantitative PCR (qPCR) assays were designed from the coding sequence (CDS) of the gene of interest (NCBI) and exon-exon junctions mapped via BLAT (42). Whenever possible, at least one of the two PCR primers was designed to transcend an exon-intron junction in order to reduce the impact of potential genomic DNA amplification in the surveyed RNA samples. Primers were designed with Primer Express 2.0 (Applied Biosystems, Foster City, CA) using default settings (primer melting temperature [$T_m$] = 58°C to 60°C, GC content = 30 to 80%, and amplicon length = 90 to 150 nucleotides). Primers were synthesized (IDT, San Jose, CA) and reconstituted to a final concentration of 100 μM (master stock) prior to dilution to a working stock of 6 μM. Primer sequences used for quantifying the gene expression levels were as follows: Stat1 forward (for), GAAA GTATTACTCCAGGCCAAAGG; Stat1 reverse (rev), TGTAAACATGTC ACTCTTCTGTGTTCA; CCL5 for, TCTACACCAGTGGCAAGTGCTC; CCL5 rev, CCCGAACCCATTTCTTCTCTG; CXCL10 for, CTTTCTGA CTCTAAGTGGCATTCAAG; CXCL10 rev, TGGATTAACAGGTTGAT TACTAATGCTG; CXCL11 for, CCTTGGCTGTGATATTGTGTGC; CXCL11 rev, GAGGCTTTCTCAATATCTGCCAC; IFIT1 for, CTGGGT ATGCGATCTCTGCC; IFIT1 rev, TTAAGCGGACAGCCTGCC; IFNB1 for, GCAGTTCCAGAAGGAGGACG; IFNB1 rev, TCCAGCCAGTGCTA GATGAATC; IL-8 for, CAGCCTTCCTGATTTCTGCAG; IL-8 rev, AGG TTTGGAGTATGTCTTTATGCACTG; ISG15 for, ATCTTTGCCAGTA CAGGAGCTTG; ISG15 rev, GACACCTGGAATTCGTTGCC; MX-1 for, GGAGGAGATCTTTCAGCACCTG; MX-1 rev, GCCGTACGTCTGGA GCATG; ephrin-B2 for, TCCAGAACTAGAAGCTGGTACAAATG; ephrin-B2 rev, GAATGTCCGGCGCTGTTG; ephrin-B3 for, GTCTGAAAT GCCCATGGAAAGA; and ephrin-B3 rev, GAGGTTGCATTGCTGG TGG. Reverse transcription was performed on 1 μg of total RNA (previously assayed via Affymetrix GeneChip) with random primers, utilizing TaqMan reverse transcription reagents (Applied Biosystems) as recommended by the manufacturer. Although the mass of input RNA should not be utilized for normalization purposes, amounts of input RNA to be assayed should be equivalent. The reverse transcription reaction was used as the template for the subsequent PCR, consisting of FastStart Universal SYBR green PCR master mix (ROX) (Roche, Indianapolis, IN), 1 μl of template cDNA, and assay primers (300 nM final concentration) in a total reaction volume of 25 μl. Thermal cycling was carried out with an ABI

Prism 7500 sequence detection system (Life Technologies, Carlsbad, CA) under factory defaults (50°C for 2 min, 95°C for 10 min, and 40 cycles at 95°C for 15 s and 60°C for 1 min). Threshold cycle ($C_T$) numbers were defined as fluorescence values, generated by SYBR green binding to double-stranded PCR products, exceeding baseline. Relative transcript levels were quantified as a comparison of measured $C_T$ values for each reaction to a designated control via the $\Delta\Delta C_T$ method (43). In order to normalize for template input, 18S rRNA (endogenous control) transcript levels were measured for each sample and utilized in these calculations. A Student *t* test was applied to 18S rRNA $C_T$ values to rule out any change in expression of the endogenous control due to treatment. Fold change values were calculated as a log 2 ratio of the $\Delta\Delta C_T$ averages of the biological replicates.

**Milliplex analysis.** Cytokine and chemokine concentrations in the supernatants of henipavirus-infected NHBE and SAEC were determined using a Milliplex Human Cytokine PREMIXED 28 Plex immunoassay kit (Millipore, Billerica, MA). Prior to analysis, samples were inactivated on dry ice by gamma radiation (5 megarads). The assay was performed according to the manufacturer's instructions. The human cytokine standards were prepared using NHBE and SAEC media. The concentrations of 28 cytokines {epidermal growth factor (EGF), granulocyte colony-stimulating factor (G-CSF), granulocyte-macrophage colony-stimulating factor (GM-CSF), IFN-α2, IFN-γ, interleukin 1α (IL-1α), IL-1β, IL-2, IL-3, IL-4, IL-5, IL-6, IL-7, IL-8, IL-10, IL-12 (p40), IL-12 (p70), IL-13, IL-15, IL-17A, chemokine ligand 3-like 1 (CCL3L1 or MIP-1α), chemokine ligand 4 (CCL4 or MIP-1β), chemokine ligand 10 (IP-10 or CXCL10), chemokine ligand 11 (CCL11 or eotaxin), chemokine ligand 13 (CCL13 or monocyte chemoattractant protein 1 [MCP-1]), tumor necrosis factor alpha (TNF-α), lymphotoxin alpha (TNF-β), and vascular endothelial growth factor A (VEGF)} were quantified.

**Western blot experiments.** To characterize the levels of IFN antagonism in henipavirus-infected NHBE and SAEC, 1,000 IU/ml of IFN-β was added for 1 h to stimulate cells at 12, 18, and 24 h postinfection. The cell lysates were then harvested, and the levels of expression of signal transducer and activator of transcription 1 (Stat1) and phosphorylated Stat1 (p-Stat1) were quantified by Western blotting. Samples were inactivated by lysis in 2× SDS lysing buffer (0.5 M Tris-HCl at pH 6.8, 20% glycerol, 10% [wt/vol] SDS, 0.1% [wt/vol] bromophenol blue, and 2-mercaptoethanol at a 5.0% final concentration) and heating for 5 min at 100°C. Proteins were run on SDS-PAGE, transferred to polyvinylidene difluoride membranes (Bio-Rad, Hercules, CA), and blocked in a Superblock buffer (Thermo Scientific, Logan, UT) before immunodetection. A rabbit polyclonal IgG was used for Stat1 p84/p91 detection (Santa Cruz Biotechnology, Santa Cruz, CA) and for p-Stat1$^{(Y701)}$ p84/p91 detection (Cell Signaling Technology, Danvers, MA). A sheep polyclonal antibody to rabbit IgG conjugated to horseradish peroxidase (HRP) was used as a secondary antibody for Stat1 and p-Stat1 detection. Beta-actin was used as loading control and was detected using a mouse monoclonal antibody directly conjugated to HRP (Abcam, Cambridge, MA). Stat1 and p-Stat1 expression levels were quantified with Quantity One Software during henipavirus infection at 12, 18, and 24 h p.i. (experiment performed in triplicate). The Stat1 and p-Stat1 intensities were corrected by dividing by the actin intensity. The pStat1/Stat1 ratio was then generated using the p-Stat1 and Stat1 corrected intensities.

**Statistical analyses.** Comparisons of virus replication levels, gene expression fold changes by qPCR assay, concentrations of cytokines and chemokines, and pStat1/Stat1 ratios were subjected to a repeated-measure one-way ANOVA in which the virus strain used (or control versus virus) was the independent variable. When the ANOVAs revealed a significant main effect, a *post hoc* test such as Bonferroni's multiple-comparison test was used to determine whether treatment means were significantly different from one another. Comparison of NiV-M or NiV-B or HeV replication levels in cells left untreated or treated with IFN was performed using the paired *t* test. All data are presented in figures as means ± standard deviations (SD).

## RESULTS

**Primary human epithelial cells derived from the bronchi and the small airway are highly susceptible to henipavirus infection.** Epithelial cells derived from the bronchi (NHBE) and the small airways (SAEC) of the human respiratory tract were investigated as potential initial sites of henipavirus replication. Both cell types expressed the henipavirus receptors ephrin-B2 and -B3, suggesting that they are permissive for infection. Gene expression of ephrin-B2 in SAEC was 2-fold higher than in NHBE. In contrast, ephrin-B3 gene expression in NHBE was 5-fold higher than in SAEC. Upon infection, both NHBE and SAEC were highly permissive to NiV-M, NiV-B, and HeV replication. Using an MOI of 5 to synchronize infection, the first cytopathic effect (CPE), characterized by syncytium formation, in infected NHBE and SAEC was observed as early as 12 to 18 h postinfection (p.i.), independent of the virus strain. NiV-infected cells showed extensive syncytium formation compared to that of HeV-infected cells at 24 h p.i. (Fig. 1A and B). NHBE and SAEC cultures infected with any of the henipavirus strains showed complete CPE by 48 h p.i. HeV and NiV replication was able to reach a high titer (greater than $10^{6.5}$ $TCID_{50}$s/ml) in both NHBE and SAEC at 32 h p.i. No significant differences between replication of the two NiV strains and HeV were observed in NHBE at any time point up to 48 h p.i. (Fig. 1C). In contrast, in SAEC, HeV replicated significantly faster up to 18 h p.i. ($10^{5.2}$ $TCID_{50}$s/ml) than did NiV-M and NiV-B ($10^{3.9}$ and $10^{3.8}$ $TCID_{50}$s/ml, respectively; $P < 0.05$).

**Study of gene expression in henipavirus-infected NHBE and SAEC.** Characterization of the global henipavirus-host interactions in SAEC and NHBE was performed by microarray analysis at 24 h p.i., a time point at which virus titers were identical for all three viruses (Fig.1C and D) and differential expression of host immune response-related genes, such as those for IL-6, MX-1, and CXCL10, was highest based on preliminary data obtained by real-time quantitative reverse transcription-PCR (qRT-PCR) assays (data not shown). A global analysis of the data by microarray showed that NiV-M induced larger numbers of differentially expressed genes in NHBE and SAEC (2,540 and 2,223, respectively) than did NiV-B (1,817 and 1,836, respectively) or HeV (2,075 and 1,642, respectively) (Fig. 2A). More than half of those differentially expressed genes in infected NHBE or SAEC were common to all 3 virus strains (Fig. 2B).

To gain more insight into the immune response against henipavirus infection in NHBE and SAEC, the most significant functional annotations were determined by Ingenuity Pathway Analysis using all differentially expressed genes per condition (i.e., NiV-M or NiV-B or HeV in NHBE or SAEC) (Fig. 3A and B). In NHBE, the data showed that NiV-M was the only virus that did not affect the expression of genes related to the antimicrobial response, the cell-mediated immune response, and immune cell trafficking. Also, NiV-M infection in NHBE affected very few genes from the inflammatory response compared to NiV-B or HeV (Fig. 3A) but triggered twice more differentially expressed genes in the infectious disease group than did NiV-B infection. In SAEC, NiV-M and NiV-B infection triggered similar numbers of differentially expressed genes related to the inflammatory response, the infectious disease, the cell-mediated immune response, and immune cell trafficking but did not modify the expression of genes related to the antimicrobial response (Fig. 3B). Finally, HeV infection triggered at least three times more differentially expressed genes related to the inflammatory response than NiV-M or NiV-B infection.

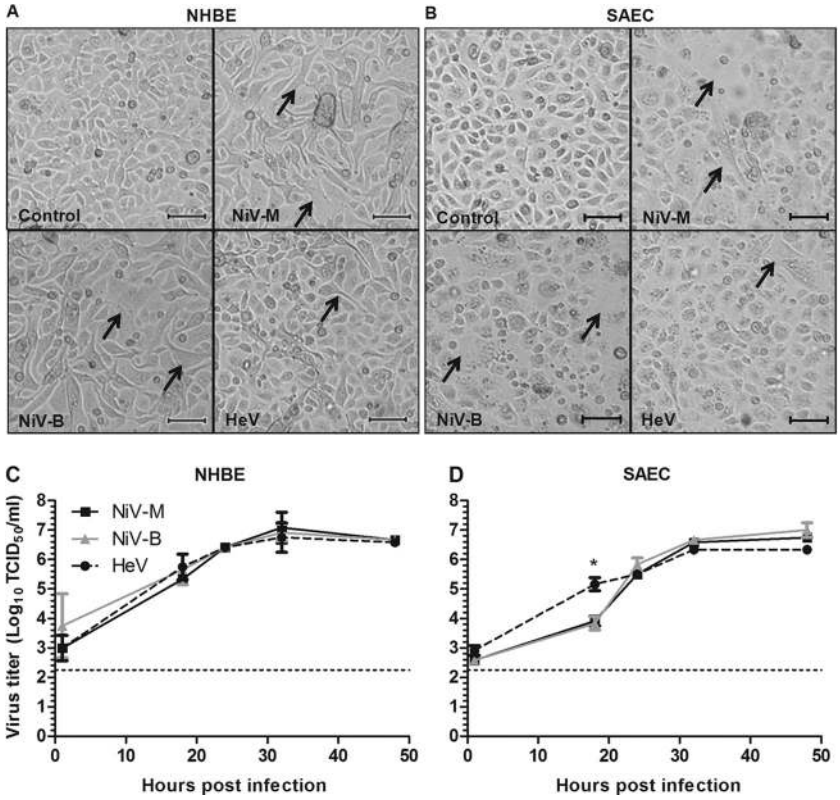


**FIG 1** Primary human epithelial cells from the respiratory tract are highly permissive to henipavirus infection. Cultures of NHBE (A and C) and SAEC (B and D) cells were infected with NiV-M, NiV-B, or HeV as described in Materials and Methods. (A and B) Syncytium formation observed at 24 h postinfection. Scale bar, 10 μm. The black arrows show syncytia in infected cells. (C and D) Kinetics of henipavirus replication in NHBE (C) and SAEC (D). Results are expressed as the average of 3 repetitions; error bars represent standard deviations. The horizontal dotted line corresponds to the detection limit. *, $P < 0.05$ by ANOVA (Bonferroni's multiple-comparison test).

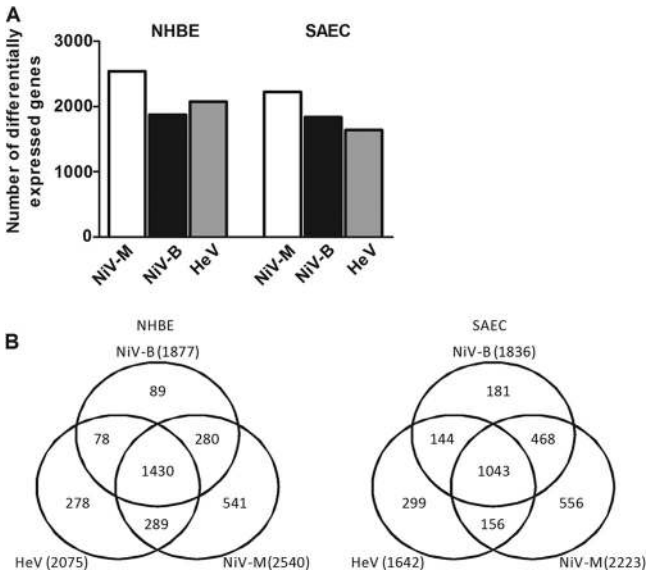


**FIG 2** Global gene expression analysis of henipavirus infection in primary epithelial cells from the respiratory tract. (A) Number of differentially expressed genes following NiV-M, NiV-B, or HeV infection in NHBE and SAEC compared to uninfected NHBE or SAEC at 24 h postinfection. Cutoff > 2; *P* value < 0.05 (right-tailed Fisher exact method). (B) Venn diagrams showing unique and common differentially expressed genes between NiV-M-, NiV-B-, and HeV-infected cells in NHBE and SAEC.

The most significant immune response-related canonical pathways were then determined using all differentially expressed genes. In NHBE, the IFN signaling pathway and the pattern recognition receptors (PRR) pathway, which included Toll-like receptor signaling and RIG-I-like receptor signaling, were in the top 10 list of the total canonical pathways affected by HeV (Fig. 3C), as with the IL-6 and IFN signaling pathways in SAEC (Fig. 3D). None of these pathways in NHBE or SAEC were reported in such a high rank or could even be considered ($P > 0.05$) using NiV-M or NiV-B (Fig. 3C and D). Surprisingly, no immune response-related canonical pathways were observed in the top 10 list of the total canonical pathways affected by NiV infection in NHBE and SAEC, with the exception of B cell receptor signaling in NiV-B-infected NHBE. In addition, the *P* values associated with IL-6 and -8 signaling during NiV-B infection in NHBE were more significant than in HeV or NiV-M infection (Fig. 3C). The *P* values associated with IL-6 and -8 signaling were significant in NiV-M infection but not during NiV-B infection in SAEC (Fig. 3D). Finally, an analysis of the differentially expressed genes that were unique to NiV-M or NiV-B infection (Fig. 2B) did not show any immune response-related canonical pathway in either NHBE or SAEC ($P > 0.05$). However, using HeV, the roles of PRR, IFN signaling, and RIG-I-like receptors in antiviral innate immunity pathway had significant *P* values in NHBE, as did IFN signaling, IL-6, GM-CSF, PRR in recognition of viruses, and the IL-17 pathway in SAEC.

Overall, the fold changes for the most upregulated immune

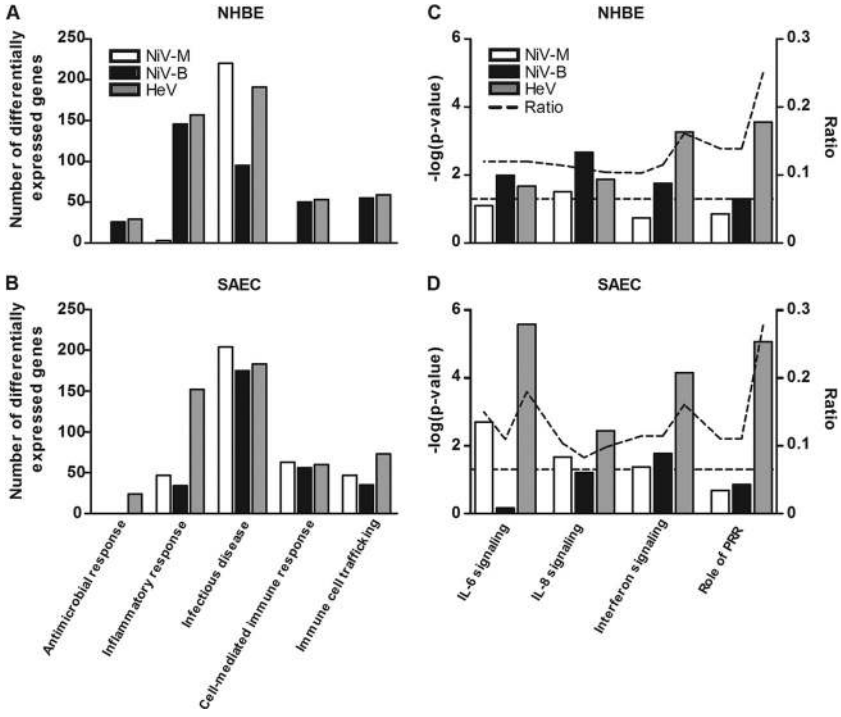


**FIG 3** Gene expression analysis of henipavirus infection in primary epithelial cells from the respiratory tract. Shown are the numbers of differentially expressed genes in the most significant biological functional groups in NHBE (A) and SAEC (B) at 24 h p.i. and the most significant biological canonical pathways in NHBE (C) and SAEC (D) at 24 h p.i. The horizontal dashed line represents the false discovery rate, fixed at 5% ($P > 0.05$), with the *P* value scale on the left *y* axis. The ratio (dashed line) is the number of overlapping genes from a particular pathway (scale on the right *y* axis).

response-related genes were higher in SAEC than in NHBE using the same virus and higher in HeV-infected than in NiV-infected cells (Table 1). These included chemokines (CCL5, CXCL10, and CXCL11), interleukins (IL-8 and IL-24A), interferon-induced proteins (IFIT1, IFIT3, MX-1, IFI6, IFI27, and IFI44L), and IFN-β1. The relative quantifications of a subset of these upregulated genes in infected NHBE and SAEC (the genes for CCL5, CXCL10, CXCL11, IFIT1, IL-8, ISG15, MX-1, Stat1, and IFN-β1) were confirmed by real-time qPCR assays (Fig. 4), which confirmed the fold change observed with the microarray data (Table 1).

**Cytokine and chemokine production by henipavirus-infected NHBE and SAEC.** The amount of a subset of cytokines and chemokines produced by henipavirus-infected NHBE and SAEC was determined to confirm the gene expression results (Fig. 5). Among a panel of 28 human cytokines and chemokines tested, only 6 cytokines (G-CSF, GM-CSF, IL-1α, IL-6, IL-8, and VEGF) plus 3 chemokines (CXCL10, MCP-1, and eotaxin) were detected in the supernatant of NHBE or SAEC at 24 h p.i. Surprisingly, genes for G-CSF and MCP-1 were not significantly expressed in the microarray analysis, while their protein expression levels in the supernatants of infected NHBE or SAEC were elevated at least 2-fold compared to those in uninfected NHBE or SAEC. This was also true for GM-CSF in NHBE and for IL-1α in SAEC. Finally, the quantities of IL-6, IL-8, VEGF, CXCL10, and eotaxin detected in the supernatant of infected cells were concomitant with their respective gene expression fold changes.

With exception of VEGF, all cytokines and chemokines were secreted at consistently higher concentrations in the supernatants of SAEC than in the supernatants of NHBE when the same virus was used. Surprisingly, no significant difference could be noticed between NiV-M and NiV-B infection in the supernatant of infected NHBE or SAEC as to the amount of cytokines and chemokines, with the exception of G-CSF and GM-CSF in NHBE ($P < 0.05$). IL-1α and CXCL10 were significantly higher in the supernatant of HeV-infected SAEC than in NiV-M- or NiV-B-infected SAEC ($P < 0.001$). This difference was also noticed in the supernatant of NHBE with CXCL10 ($P < 0.001$). Conversely,MCP-1 was the only selected chemokine that was at a lower concentration in the supernatant of HeV-infected SAEC than in the supernatant of NiV-infected SAEC.

**Type I interferon pretreatment of epithelial cells derived from the bronchi and the small airway can limit henipavirus replication.** Since NiV and HeV have been shown to counteract the innate immune response and particularly the type I interferon (IFN) response, the effect of IFN treatment on virus replication in NHBE and SAEC was assessed (Fig. 6). Cells were treated with 1,000 IU/ml of IFN-β for 24 h prior to infection. IFN treatment of NHBE cells resulted in complete inhibition of NiV-M and NiV-B replication, while low levels of HeV replication were observed at 32 h p.i. ($10^{3.7}$, $10^{3.5}$, and $10^{4.8}$ $TCID_{50}$s/ml for NiV-M, NiV-B, and HeV, respectively; $P > 0.05$). The mean virus titer of HeV, NiV-M, and NiV-B at 32 h p.i. was decreased by 2 to 3 log units ($P > 0.05$) in NHBE pretreated with IFN. IFN treatment of SAEC delayed both NiV-M and HeV replication up to 32 h, while NiV-B replication was observed as early as 24 h p.i. ($10^{3.4}$, $10^{4.7}$, and $10^{3.6}$ $TCID_{50}$s/ml for NiV-M, NiV-B, and HeV, respectively; $P < 0.001$). The mean virus titer of NiV-M, NiV-B, or HeV at 32 h p.i. was decreased 1 to 2 log units ($P < 0.05$) in IFN-treated SAEC.

**TABLE 1** Top upregulated genes in the immune response and interferon signaling of infected cells

| Name | Gene identity for humans | Description | Fold change | | | | | | Function |
|---|---|---|---|---|---|---|---|---|---|
| | | | NiV-M | | NiV-B | | HeV | | |
| | | | NHBE | SAEC | NHBE | SAEC | NHBE | SAEC | |
| CXCL11 | 6373 | Chemokine (C-X-C motif) ligand 11 | 27.9 | 147.6 | 24.5 | 114.6 | 70.4 | 309.9 | Immune response |
| CTH | 1491 | Cystathionase (cystathionine gamma-lyase) | 17.0 | 3.8 | 16.1 | 2.6 | 15.7 | 3.8 | Immune response |
| IL13RA2 | 3598 | Interleukin 13 receptor, alpha 2 | 13.7 | 6.8 | 18.8 | 12.2 | 12.7 | 10.2 | Immune response |
| TSLP | 85480 | Thymic stromal lymphopoietin | 11.3 | 11.3 | 13.4 | 10.1 | 9.7 | 12.0 | Immune response |
| ISG15 | 9636 | ISG15 ubiquitin-like modifier | 9.1 | 23.1 | 8.6 | 15.3 | 21.5 | 27.8 | Immune response |
| ATF3 | 467 | Activating transcription factor 3 | 4.2 | 4.0 | 4.3 | 4.7 | 5.2 | 9.4 | Immune response |
| CXCL2 | 2920 | Chemokine (C-X-C motif) ligand 2 | 4.1 | | 6.2 | | 10.2 | 4.6 | Immune response |
| CXCL10 | 3627 | Chemokine (C-X-C motif) ligand 10 | 3.8 | 5.0 | 3.7 | 3.8 | 16.4 | 39.8 | Immune response |
| BIRC3 | 330 | Baculoviral IAP repeat containing 3 | 3.6 | 6.8 | 4.9 | 11.2 | 6.0 | 12.7 | Immune response |
| CCL5 | 6352 | Chemokine (C-C motif) ligand 5 | 2.5 | 14.1 | 2.1 | 7.5 | 2.2 | 17.1 | Immune response |
| IL28A | 282616 | Interleukin 28A (interferon, lambda 2) | 2.4 | | | | | 10.2 | Immune response |
| IFI6 | 2537 | Alpha interferon-inducible protein 6 | 2.2 | 5.0 | 3.9 | 7.4 | 20.7 | 20.3 | Immune response |
| IFI44L | 10964 | Interferon-induced protein 44-like | 2.1 | | 2.0 | | 18.2 | 10.6 | Immune response |
| IL-8 | 3576 | Interleukin 8 | | | 2.0 | 4.9 | 2.4 | 7.4 | Immune response |
| OAS2 | 4939 | 2′,5′-Oligoadenylate synthetase 2, 69/71 kDa | | 2.2 | 2.6 | 2.1 | 9.7 | 6.3 | Immune response |
| IL-24 | 11009 | Interleukin 24 | | 4.4 | | 10.3 | | 3.7 | Immune response |
| IFI27 | 3429 | Alpha interferon-inducible protein 27 | | 2.4 | 2.1 | 3.5 | 6.6 | 9.5 | Immune response |
| ISG20 | 3669 | Interferon-stimulated exonuclease gene, 20 kDa | | 8.1 | 2.9 | 7.3 | 3.3 | 8.6 | Immune response |
| CXCL3 | 2921 | Chemokine (C-X-C motif) ligand 3 | | 2 | | | 3.4 | 11.5 | Immune response |
| IFIT1 | 3434 | Interferon-induced protein with tetratricopeptide repeats 1 | 19.2 | 131.4 | 21.5 | 95.1 | 42.5 | 171.0 | Interferon signaling |
| IFIT3 | 3437 | Interferon-induced protein with tetratricopeptide repeats 3 | 4.6 | 17.4 | 5.1 | 12.5 | 11.2 | 21.7 | Interferon signaling |
| Stat1 | 6772 | Signal transducer and activator of transcription 1 | −2.5 | | | | 4.7 | 2.0 | Interferon signaling |
| OAS1 | 4938 | 2′,5′-Oligoadenylate synthetase 1 | | | 2.0 | | 4.6 | 3.2 | Interferon signaling |
| MX1 | 4599 | Myxovirus (influenza virus) resistance 1, interferon-inducible protein p78 (mouse) | | | 2.2 | | 10.4 | 7.7 | Interferon signaling |
| IFN-β1 | 3456 | Beta 1 interferon | | 5.3 | | 2.7 | 2.1 | 18.3 | Interferon signaling |
| IFI35 | 3430 | Interferon-induced protein 35 | | | | | 2.6 | 2.6 | Interferon signaling |
| IFITM1 | 8519 | Interferon-induced transmembrane protein 1 | | | | 2.8 | 6.8 | | Interferon signaling |

**Characterization of the interferon immune response in henipavirus-infected NHBE and SAEC.** Based on the microarray results, the interferon signaling pathway was one of the most significant canonical pathways affected by HeV but not by NiV infection in both NHBE and SAEC at 24 h p.i. The ability of HeV and NiV strains to antagonize the interferon signaling was thus assessed in time by quantifying the amount of phosphorylated Stat1 (p-Stat1). The levels of beta-actin and Stat1 during henipavirus infection in NHBE or SAEC did not significantly change compared to their respective levels in uninfected cells at 12, 18, and 24 h p.i. (data not shown). However, henipavirus infection of NHBE and SAEC resulted in a significant reduction in p-Stat1 induction following a 1-h treatment with 1,000 IU/ml of IFN-β compared to uninfected controls (Fig. 7). No significant difference in p-Stat1 induction between the 3 virus strains was observed at 12 h p.i. Interestingly, activation of p-Stat1 was completely blocked by NiV-M as early as 18 h p.i. (p-Stat1/Stat1 ratio of 0) but not by NiV-B or HeV ($P < 0.001$). The quantity of p-Stat1 in NiV-B- or HeV-infected cells (p-Stat1/Stat1 ratios of 1.0 and 1.1 in NHBE, respectively, and of 0.8 and 0.9 in SAEC, respectively) was, however, at that time reduced by about 2 compared to the quantity of p-Stat1 in uninfected NHBE or SAEC (p-Stat1/Stat1 ratios of 1.9 and 2.1, respectively; $P < 0.001$). Finally, no p-Stat1 could be detected in any of the henipavirus-infected cells at 24 h p.i. (p-Stat1/Stat1 ratio of 0), while the ratios in uninfected NHBE or SAEC were equal to 1.2 and 1.0, respectively ($P < 0.001$).

## DISCUSSION

Hendra and Nipah viruses are newly emerging zoonotic viruses that can cause severe respiratory illness and encephalitis in humans. Despite intensive studies, little is known about the early stages of henipavirus infection in the human respiratory tract. Here we report the establishment and characterization of NiV and HeV infection in human respiratory epithelium using undifferentiated primary epithelial cell monolayers derived from bronchi and small airways to study the role of the host responses in pathogenesis.

The epithelial cells derived from the bronchi (NHBE) and the small airways (SAEC) of the human respiratory tract were highly susceptible to NiV and HeV infection, as characterized by high peak titers and characteristic syncytium formation as early as 12 h p.i. Although HeV initially replicated faster than NiV-M and NiV-B in the small airways, all virus strains reached similar peaks of replication as early as 32 h p.i. in both cell types, making them likely targets for virus infection during natural infection. The efficient replication of HeV in bronchus-derived epithelial cells was surprising, as we previously observed that HeV antigen could not be detected in the epithelium of trachea and bronchi of infected

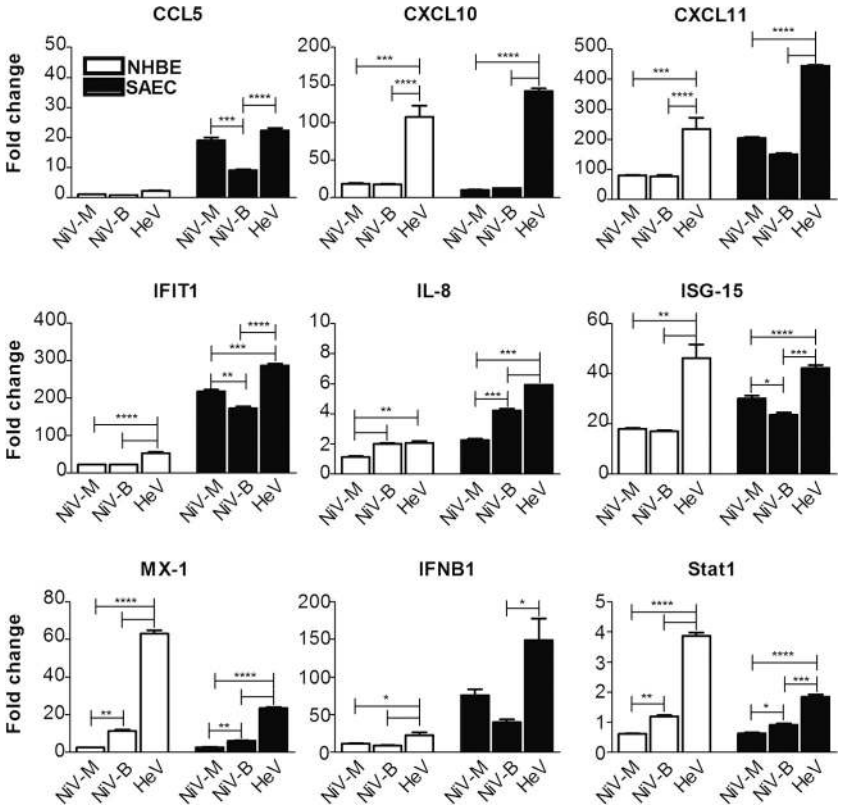


**FIG 4** Expression of the most upregulated genes of the immune response and interferon signaling in henipavirus-infected NHBE and SAEC. Shown is real-time qPCR analysis of the expression of CCL5, CXCL10, CXCL11, IFIT1, IL-8, ISG-15, MX-1, IFN-β1, and Stat1 compared to noninfected NHBE or SAEC at 24 h postinfection. Results are expressed as the averages of 3 repetitions, and bars represent standard deviations. *, $P < 0.05$; **, $P < 0.01$; ***, $P < 0.001$; ****, $P < 0.0001$ (ANOVA; Bonferroni's multiple-comparison test).

hamsters, suggesting limited replication in these cells (34). One explanation is that this observation is species specific. Another key difference is the fact that we used undifferentiated epithelial cells in the current study. The conditions present in tissue culture result in a dedifferentiation and subsequent loss of beating cilia, which may affect virus entry and replication by an unidentified mechanism. Studies of the role of epithelial differentiation in virus susceptibility and host responses are ongoing. Both NHBE and SAEC types have previously been used as *in vitro* models to study a variety of respiratory viruses, including other members of the *Paramyxoviridae* family such as measles virus and respiratory syncytial virus (44, 45). Overall, these data suggest that human epithelial cells derived from the bronchi and the small airways are highly relevant to study henipavirus replication in the respiratory epithelium.

The global analysis of host gene expression revealed two major characteristics. First, henipavirus infection of SAEC resulted in higher fold changes in host gene expression than obtained with NHBE, suggesting that epithelial cells derived from different areas of the human respiratory tract respond differentially to henipavirus infection. This result is in line with the observations that NiV infection in humans cases, as well as in hamsters, resulted in inflammation of the small airways but not the bronchi (29, 34). Second, infection of NHBE and SAEC with NiV-M, NiV-B, and HeV resulted in differences in induction of host immune response between these genetically distinct henipavirus strains. Overall, host responses were higher in HeV-infected cells than in cells infected with either NiV strain. Specifically, NiV-M infection in NHBE resulted in differential expression of very few genes related to the inflammatory response compared to results obtained with NiV-B or HeV. This is in agreement with the observation that no inflammation occurred in the epithelium of bronchi in NiV-M-infected patients (29) and suggests that inflammation may occur in the bronchi of NiV-B- or HeV-infected patients even though no histopathological changes have been reported so far in this area. Our data clearly showed that key inflammatory mediators, including IL-6, IL-8, CXCL10, MCP-1, and CCL5, were highly upregulated in SAEC but not in NHBE infected with henipavirus. Interestingly, HeV induced higher levels of these cytokines and chemokines than did both NiV strains, with the exception of MCP-1. IL-6, which is released by epithelial cells and macrophages in the respiratory tract, promotes pulmonary inflammation, and high levels in bronchoalveolar lavage fluid and in serum are correlated with severity and mortality of acute respiratory distress syndrome (ARDS) (46, 47) and with severe disease, including respiratory insufficiency in pandemic H1N1 influenza virus-infected patients (48, 49), respectively. In addition, inhibition of IL-6 reduces lung injury in mice with acute kidney injury by reducing the levels of IL-8 and neutrophil influx in the lung (50). In line with the previous statement, IL-8 has also been shown to control neutrophil-mediated inflammation during rhinovirus infection (51) and to contribute in the pathogenesis of ARDS (52–55), and it was recently reported at elevated levels in serum of H5N1-infected patients, especially in those who succumbed to the

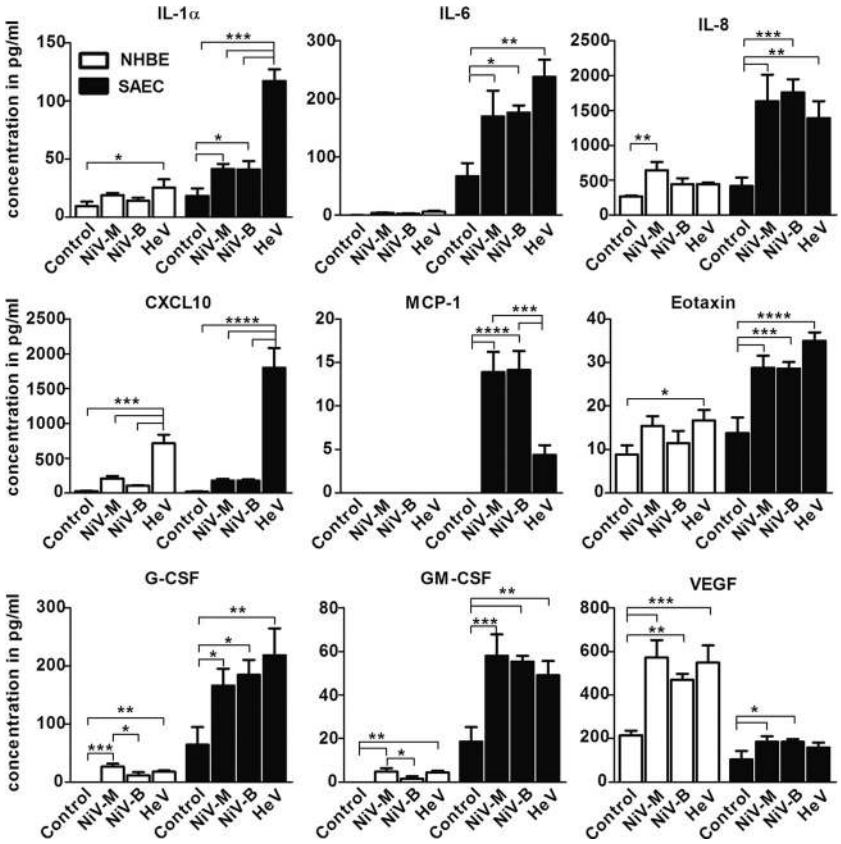


**FIG 5** Quantification of the principal cytokines and chemokines secreted in the supernatants of NHBE and SAEC at 24 h p.i. Cytokines and chemokines were quantified in infected or uninfected cells as described in Materials and Methods. Results are expressed as the averages of 3 repetitions, and bars represent standard deviations. *, $P < 0.05$; **, $P < 0.01$; ***, $P < 0.001$; ****, $P < 0.0001$ (ANOVA; Bonferroni's multiple-comparison test.

infection due to respiratory insufficiency (56). Therefore, our data suggest that IL-6 and IL-8 play important roles in inflammation of the small airways due to an increased neutrophil influx in the small airways, as observed in NiV-M-infected dogs (57) and in HeV-infected swine (58), compared to the bronchi. Chemokines such as CXCL10 and MCP-1 are macrophage chemoattractants and, along with CCL5, recruit circulating leukocytes to the inflamed tissue. Overexpression of CXCL10 has previously been reported to occur in the lung of NiV-M- and HeV-infected hamsters and correlated with the influx of inflammatory cells (34, 59). Its gene expression level in the lungs of HeV-infected hamsters was also higher than in NiV-infected hamsters (34), corroborating our observations in infected NHBE and SAEC. Even though it has been shown that MCP-1 can be released from bronchial epithelium and contributes to the inflammatory pathology of bronchial asthma (60), in the current study, MCP-1 was expressed in in-

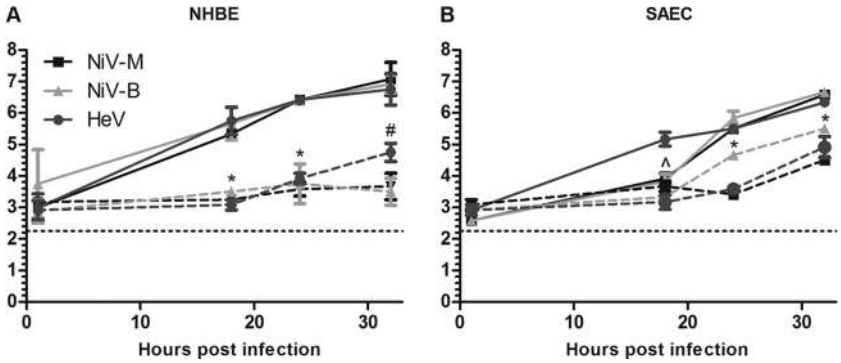


**FIG 6** Type I interferon pretreatment of epithelial cells from the bronchi and the small airways can limit henipavirus replication. Shown are the kinetics of virus replication in NHBE (A) and SAEC (B) left untreated (solid lines) or pretreated with 1,000 IU/ml of IFN-β1 for 24 h prior to infection (dashed lines). Results are expressed as the averages of 3 repetitions, with standard deviations. The horizontal dashed line corresponds to the detection limit. The symbols *, #, and ∧ correspond to significant differences of virus replication levels between untreated and IFN-treated cells using the same strain, using both NiV strains and HeV, respectively ($P < 0.05$; paired *t* test).

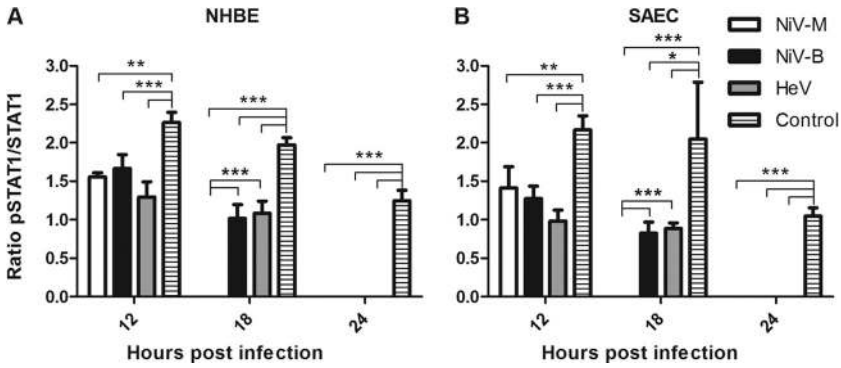


**FIG 7** Expression and activation of Stat1 during henipavirus infection in human primary epithelial cells from the respiratory tract. Prior to protein harvesting, all cells were treated with 1,000 IU/ml of IFN-β1 for 1 h (see Materials and Methods). The experiment was performed in triplicate. The Stat1 and phosphorylated Stat1 were detected by Western blotting, and the intensities were corrected using the beta-actin loading control. The p-Stat1/Stat1 ratios in uninfected and infected cells are plotted in panels A and B for NHBE and SAEC, respectively. *, $P < 0.05$; **, $P < 0.01$; ***, $P < 0.001$ (ANOVA; Bonferroni's multiple-comparison test).

fected SAEC only. Similarly, CCL5 gene expression was also mainly observed in infected SAEC, especially during HeV infection, which suggests altogether an important role of macrophage and circulating leukocyte recruitment in the small airways, leading to a larger inflammatory response than in the bronchi. These results are in agreement with histopathological changes observed in the lungs of 2 HeV-infected patients showing either an acute pulmonary syndrome with intra-alveolar macrophages and other inflammatory cells in the small airways (28) or focal necrotizing alveolitis with an influx of macrophages as well (40). This is also in line with the high levels of the inflammatory cytokine IL-1α and granulocyte-stimulating factor (G-CSF and GM-CSF) secreted in the supernatant of infected SAEC and, again, mostly during HeV infection.

In addition to uncovering the role of several key regulators of inflammation, microarray data also revealed differential gene expression in the signaling pathway of pattern recognition receptor (PRR) activation in NiV-B- and HeV-infected cells but not with NiV-M. The RIG-I-like receptor pathway was activated during HeV infection, suggesting that type I interferon was expressed in infected cells. This was confirmed by the increased IFN-β gene expression in all infected cells, mainly in SAEC and especially during HeV infection, which was in line with the activation of the IFN-α/β signaling pathway in HeV-infected cells. Consequently, higher levels of interferon-induced gene expression such as for IFIT1, IFIT3, MX-1, ISG-15, and IFIT35 were observed in HeV-infected cells than in NiV-infected cells. Surprisingly, the high expression of CXCL10 in HeV-infected cells was independent of gamma interferon induction and could be the result of a direct viral activation of steps in the interferon pathway (61–63). Interestingly, while NiV and HeV infection resulted in complete inhibition of Stat1 activation at 24 h p.i., NiV-M was more efficient at blocking Stat1 activation at earlier time points than were NiV-B and HeV. This result is in line with the differences of NiV-M replication levels in untreated cellular models and with pretreatment with IFN type I, which were higher than the levels of HeV, suggesting a more important role of IFN response blocking to satisfy NiV-M replication. Since growth kinetics for all three viruses were similar, it is likely that the viral proteins P, V, and W, which can each inhibit phosphorylation of Stat1 (64–69), differentially affect the IFN pathway dependent on the virus strain. This differential induction of the IFN response may, in turn, affect virulence through an unknown mechanism, as suggested for a recently discovered henipavirus, Cedar virus (70), as well as for influenza viruses. The nonstructural NS1 protein of influenza virus is the main viral IFN antagonist, and NS1 proteins of more virulent strains were recently reported as having a higher interferon type I signaling inhibitory activity *in vitro* as well as contributing to a more persistent infection in the upper and lower respiratory tracts of ferrets (71). In outbreaks, the NiV-M strain has been less virulent than the NiV-B strain despite an increased ability to block interferon type I signaling *in vitro*. In various animal models, such as hamsters, ferrets, and African green monkeys, HeV has consistently been more virulent than NiV-M and NiV-B despite being more sensitive to IFN (unpublished data). Interestingly, a NiV-M strain lacking either the C or V protein did not cause any clinical signs in hamsters, which was possibly due to a reduced replication ability as observed *in vitro* (72). These results suggest that viral proteins with IFN antagonist functions can influence the virulence, although the exact role of interferon antagonism in the pathogenesis of henipaviruses remains unclear.

Finally, the high level of secreted VEGF, as observed in the supernatant of infected NHBE, may play a role in airway remodeling, a phenomenon previously observed during rhinovirus-associated asthma exacerbations (73). The monolayer NHBE used in this study define a simplified model but if relevant *in vivo*, the VEGF overexpression might affect the subjacent endothelial cells and lead to vascular leakage and increased permeability (74). This is part of ongoing studies using a more complex *in vitro* model including both epithelial and endothelial cells. To our knowledge, there is no study reporting a role for VEGF during henipavirus infection or a remodeling of the respiratory tract in infected animals and in human cases. Its function in the respiratory tract, and particularly in the bronchi, in facilitating henipavirus dissemination into the vascular system is still unknown and requires further investigations.

In conclusion, our data show that henipaviruses are able to efficiently replicate in epithelial cells derived from the bronchi and the small airways of the human respiratory tract. Infection of these cells results in a higher inflammatory response in SAEC than in NHBE, especially during HeV infection, including key inflammatory mediators: IL-6, IL-8, IL-1α, MCP-1, G-CSF, GM-CSF, and

CXCL10. Finally, we demonstrate a virus strain-dependent variability in type I IFN signaling. This study demonstrates that primary human epithelial cells derived from the bronchi and the small airways serve as an important site of HeV and NiV replication, suggesting that both viruses have the potential for human-to-human transmission through aerosols. We believe that these models allow for more detailed studies of the pathogenesis of respiratory disease caused by HeV and NiV infection in humans. These data provide several target genes and pathways that potentially play roles in henipavirus pathogenesis which will be valuable as candidates for future studies of the mechanism of henipavirus pathogenesis and as potential targets for treatment.

## ACKNOWLEDGMENTS

The study was funded by University of Texas Medical Branch startup funds and by the Intramural Research Program, NIAID, NIH. We also thank the Philippe Foundation for financial support to O.E.

We thank Alisha Prather for critical review of the manuscript.

## REFERENCES

1. **Eaton BT, Broder CC, Wang LF.** 2005. Hendra and Nipah viruses: pathogenesis and therapeutics. Curr. Mol. Med. **5**:805–816.
2. **Murray K, Selleck P, Hooper P, Hyatt A, Gould A, Gleeson L, Westbury H, Hiley L, Selvey L, Rodwell B, Ketterer P.** 1995. A morbillivirus that caused fatal disease in horses and humans. Science **268**:94–97.
3. **O'Sullivan JD, Allworth AM, Paterson DL, Snow TM, Boots R, Gleeson LJ, Gould AR, Hyatt AD, Bradfield J.** 1997. Fatal encephalitis due to novel paramyxovirus transmitted from horses. Lancet **349**:93–95.
4. **Rogers RJ, Douglas IC, Baldock FC, Glanville RJ, Seppanen KT, Gleeson LJ, Selleck PN, Dunn KJ.** 1996. Investigation of a second focus of equine morbillivirus infection in coastal Queensland. Aust. Vet. J. **74**: 243–244.
5. **Williamson MM, Torres-Velez FJ.** 2010. Henipavirus: a review of laboratory animal pathology. Vet. Pathol. **47**:871–880.
6. **Rockx B, Winegar R, Freiberg AN.** 2012. Recent progress in henipavirus research: molecular biology, genetic diversity, animal models. Antiviral Res. **95**:135–149.
7. **Chua KB, Bellini WJ, Rota PA, Harcourt BH, Tamin A, Lam SK, Ksiazek TG, Rollin PE, Zaki SR, Shieh W, Goldsmith CS, Gubler DJ, Roehrig JT, Eaton B, Gould AR, Olson J, Field H, Daniels P, Ling AE, Peters CJ, Anderson LJ, Mahy BW.** 2000. Nipah virus: a recently emergent deadly paramyxovirus. Science **288**:1432–1435.
8. **Goh KJ, Tan CT, Chew NK, Tan PS, Kamarulzaman A, Sarji SA, Wong KT, Abdullah BJ, Chua KB, Lam SK.** 2000. Clinical features of Nipah virus encephalitis among pig farmers in Malaysia. N. Engl. J. Med. **342**: 1229–1235.
9. **Harit AK, Ichhpujani RL, Gupta S, Gill KS, Lal S, Ganguly NK, Agarwal SP.** 2006. Nipah/Hendra virus outbreak in Siliguri, West Bengal, India in 2001. Indian J. Med. Res. **123**:553–560.
10. **Hossain MJ, Gurley ES, Montgomery JM, Bell M, Carroll DS, Hsu VP, Formenty P, Croisier A, Bertherat E, Faiz MA, Azad AK, Islam R, Molla MA, Ksiazek TG, Rota PA, Comer JA, Rollin PE, Luby SP, Breiman RF.** 2008. Clinical presentation of Nipah virus infection in Bangladesh. Clin. Infect. Dis. **46**:977–984.
11. **Anonymous.** 2012. Nipah encephalitis, human—Bangladesh: (Jipurhat). ProMED-mail 2012. 12 February 2012, archive no. 20120212.1040138. http://www.promedmail.org/direct.php?id=20120212.1040138.
12. **Lo MK, Lowe L, Hummel KB, Sazzad HM, Gurley ES, Hossain MJ, Luby SP, Miller DM, Comer JA, Rollin PE, Bellini WJ, Rota PA.** 2012. Characterization of Nipah virus from outbreaks in Bangladesh, 2008–2010. Emerg. Infect. Dis. **18**:248–255.
13. **Chong HT, Kunjapan SR, Thayaparan T, Tong J, Petharunam V, Jusoh MR, Tan CT.** 2002. Nipah encephalitis outbreak in Malaysia, clinical features in patients from Seremban. Can. J. Neurol. Sci. **29**:83–87.
14. **Marsh GA, Wang LF.** 2012. Hendra and Nipah viruses: why are they so deadly? Curr. Opin. Virol. **2**:242–247.
15. **Chua KB, Koh CL, Hooi PS, Wee KF, Khong JH, Chua BH, Chan YP, Lim ME, Lam SK.** 2002. Isolation of Nipah virus from Malaysian Island flying-foxes. Microbes Infect. **4**:145–151.
16. **Halpin K, Young PL, Field HE, Mackenzie JS.** 2000. Isolation of Hendra virus from pteropid bats: a natural reservoir of Hendra virus. J. Gen. Virol. **81**:1927–1932.
17. **Yob JM, Field H, Rashdi AM, Morrissy C, van der Heide B, Rota P, Abin Adzhar White J, Daniels P, Jamaluddin A, Ksiazek T.** 2001. Nipah virus infection in bats (order Chiroptera) in peninsular Malaysia. Emerg. Infect. Dis. **7**:439–441.
18. **Ali R, Mounts AW, Parashar UD, Sahani M, Lye MS, Isa MM, Balathevan K, Arif MT, Ksiazek TG.** 2001. Nipah virus among military personnel involved in pig culling during an outbreak of encephalitis in Malaysia, 1998–1999. Emerg. Infect. Dis. **7**:759–761.
19. **Parashar UD, Sunn LM, Ong F, Mounts AW, Arif MT, Ksiazek TG, Kamaluddin MA, Mustafa AN, Kaur H, Ding LM, Othman G, Radzi HM, Kitsutani PT, Stockton PC, Arokiasamy J, Gary HE, Jr, Anderson LJ.** 2000. Case-control study of risk factors for human infection with a new zoonotic paramyxovirus, Nipah virus, during a 1998-1999 outbreak of severe encephalitis in Malaysia. J. Infect. Dis. **181**:1755–1759.
20. **Playford EG, McCall B, Smith G, Slinko V, Allen G, Smith I, Moore F, Taylor C, Kung YH, Field H.** 2010. Human Hendra virus encephalitis associated with equine outbreak, Australia, 2008. Emerg. Infect. Dis. **16**: 219–223.
21. **Premalatha GD, Lye MS, Ariokasamy J, Parashar UD, Rahmat R, Lee BY, Ksiazek TG.** 2000. Assessment of Nipah virus transmission among pork sellers in Seremban, Malaysia. Southeast Asian J. Trop. Med. Public Health **31**:307–309.
22. **Sahani M, Parashar UD, Ali R, Das P, Lye MS, Isa MM, Arif MT, Ksiazek TG, Sivamoorthy M.** 2001. Nipah virus infection among abattoir workers in Malaysia, 1998–1999. Int. J. Epidemiol. **30**:1017–1020.
23. **Selvey L, Sheridan J.** 1995. Outbreak of severe respiratory disease in humans and horses due to a previously unrecognized paramyxovirus. J. Travel Med. **2**:275.
24. **Lo MK, Rota PA.** 2008. The emergence of Nipah virus, a highly pathogenic paramyxovirus. J. Clin. Virol. **43**:396–400.
25. **Gurley ES, Montgomery JM, Hossain MJ, Bell M, Azad AK, Islam MR, Molla MA, Carroll DS, Ksiazek TG, Rota PA, Lowe L, Comer JA, Rollin P, Czub M, Grolla A, Feldmann H, Luby SP, Woodward JL, Breiman RF.** 2007. Person-to-person transmission of Nipah virus in a Bangladeshi community. Emerg. Infect. Dis. **13**:1031–1037.
26. **Hsu VP, Hossain MJ, Parashar UD, Ali MM, Ksiazek TG, Kuzmin I, Niezgoda M, Rupprecht C, Bresee J, Breiman RF.** 2004. Nipah virus encephalitis reemergence, Bangladesh. Emerg. Infect. Dis. **10**:2082–2087.
27. **Chua KB, Lam SK, Tan CT, Hooi PS, Goh KJ, Chew NK, Tan KS, Kamarulzaman A, Wong KT.** 2000. High mortality in Nipah encephalitis is associated with presence of virus in cerebrospinal fluid. Ann. Neurol. **48**:802–805.
28. **Wong KT, Robertson T, Ong BB, Chong JW, Yaiw KC, Wang LF, Ansford AJ, Tannenberg A.** 2009. Human Hendra virus infection causes acute and relapsing encephalitis. Neuropathol. Appl. Neurobiol. **35**:296–305.
29. **Wong KT, Shieh WJ, Kumar S, Norain K, Abdullah W, Guarner J, Goldsmith CS, Chua KB, Lam SK, Tan CT, Goh KJ, Chong HT, Jusoh R, Rollin PE, Ksiazek TG, Zaki SR.** 2002. Nipah virus infection: pathology and pathogenesis of an emerging paramyxoviral zoonosis. Am. J. Pathol. **161**:2153–2167.
30. **Hooper P, Zaki S, Daniels P, Middleton D.** 2001. Comparative pathology of the diseases caused by Hendra and Nipah viruses. Microbes Infect. **3**:315–322.
31. **Bossart KN, Rockx B, Feldmann F, Brining D, Scott D, Lacasse R, Geisbert JB, Feng YR, Chan YP, Hickey AC, Broder CC, Feldmann H, Geisbert TW.** 2012. A Hendra virus G glycoprotein subunit vaccine protects African green monkeys from Nipah virus challenge. Sci. Transl. Med. **4**:146ra107. doi:10.1126/scitranslmed.3004241.
32. **Maisner A, Neufeld J, Weingartl H.** 2009. Organ- and endotheliotropism of Nipah virus infections in vivo and in vitro. Thromb. Haemost. **102**: 1014–1023.
33. **Rockx B, Bossart KN, Feldmann F, Geisbert JB, Hickey AC, Brining D, Callison J, Safronetz D, Marzi A, Kercher L, Long D, Broder CC, Feldmann H, Geisbert TW.** 2010. A novel model of lethal Hendra virus infection in African green monkeys and the effectiveness of ribavirin treatment. J. Virol. **84**:9831–9839.
34. **Rockx B, Brining D, Kramer J, Callison J, Ebihara H, Mansfield K, Feldmann H.** 2011. Clinical outcome of henipavirus infection in hamsters is determined by the route and dose of infection. J. Virol. **85**:7658–7671.

35. **Weingartl HM, Berhane Y, Czub M.** 2009. Animal models of henipavirus infection: a review. Vet. J. **181**:211–220.
36. **Chua KB, Lam SK, Goh KJ, Hooi PS, Ksiazek TG, Kamarulzaman A, Olson J, Tan CT.** 2001. The presence of Nipah virus in respiratory secretions and urine of patients during an outbreak of Nipah virus encephalitis in Malaysia. J. Infect. **42**:40–43.
37. **Mounts AW, Kaur H, Parashar UD, Ksiazek TG, Cannon D, Arokiasamy JT, Anderson LJ, Lye MS.** 2001. A cohort study of health care workers to assess nosocomial transmissibility of Nipah virus, Malaysia, 1999. J. Infect. Dis. **183**:810–813.
38. **Tan CT, Tan KS.** 2001. Nosocomial transmissibility of Nipah virus. J. Infect. Dis. **184**:1367.
39. **Paton NI, Leo YS, Zaki SR, Auchus AP, Lee KE, Ling AE, Chew SK, Ang B, Rollin PE, Umapathi T, Sng I, Lee CC, Lim E, Ksiazek TG.** 1999. Outbreak of Nipah-virus infection among abattoir workers in Singapore. Lancet **354**:1253–1256.
40. **Selvey LA, Wells RM, McCormack JG, Ansford AJ, Murray K, Rogers RJ, Lavercombe PS, Selleck P, Sheridan JW.** 1995. Infection of humans and horses by a newly described morbillivirus. Med. J. Aust. **162**:642–645.
41. **Reed LJ, Muench H.** 1938. A simple method of estimating fifty percent endpoints. Am. J. Hyg. **27**:493–497.
42. **Kent WJ.** 2002. BLAT—the BLAST-like alignment tool. Genome Res. **12**:656–664.
43. **Livak KJ, Schmittgen TD.** 2001. Analysis of relative gene expression data using real-time quantitative PCR and the 2(-Delta Delta C(T)) method. Methods **25**:402–408.
44. **Mochizuki H, Todokoro M, Arakawa H.** 2009. RS virus-induced inflammation and the intracellular glutathione redox state in cultured human airway epithelial cells. Inflammation **32**:252–264.
45. **Takeuchi K, Miyajima N, Nagata N, Takeda M, Tashiro M.** 2003. Wild-type measles virus induces large syncytium formation in primary human small airway epithelial cells by a SLAM(CD150)-independent mechanism. Virus Res. **94**:11–16.
46. **Headley AS, Tolley E, Meduri GU.** 1997. Infections and the inflammatory response in acute respiratory distress syndrome. Chest **111**:1306–1321.
47. **Lin WC, Lin CF, Chen CL, Chen CW, Lin YS.** 2010. Prediction of outcome in patients with acute respiratory distress syndrome by bronchoalveolar lavage inflammatory mediators. Exp. Biol. Med. (Maywood) **235**:57–65.
48. **Bermejo-Martin JF, Ortiz de Lejarazu R, Pumarola T, Rello J, Almansa R, Ramirez P, Martin-Loeches I, Varillas D, Gallegos MC, Seron C, Micheloud D, Gomez JM, Tenorio-Abreu A, Ramos MJ, Molina ML, Huidobro S, Sanchez E, Gordon M, Fernandez V, Del Castillo A, Marcos MA, Villanueva B, Lopez CJ, Rodriguez-Dominguez M, Galan JC, Canton R, Lietor A, Rojo S, Eiros JM, Hinojosa C, Gonzalez I, Torner N, Banner D, Leon A, Cuesta P, Rowe T, Kelvin DJ.** 2009. Th1 and Th17 hypercytokinemia as early host response signature in severe pandemic influenza. Crit. Care **13**:R201. doi:10.1186/cc8208.
49. **Paquette SG, Banner D, Zhao Z, Fang Y, Huang SS, Leomicronn AJ, Ng DC, Almansa R, Martin-Loeches I, Ramirez P, Socias L, Loza A, Blanco J, Sansonetti P, Rello J, Andaluz D, Shum B, Rubino S, de Lejarazu RO, Tran D, Delogu G, Fadda G, Krajden S, Rubin BB, Bermejo-Martin JF, Kelvin AA, Kelvin DJ.** 2012. Interleukin-6 is a potential biomarker for severe pandemic H1N1 influenza A infection. PLoS One **7**:e38214. doi:10.1371/journal.pone.0038214.
50. **Klein CL, Hoke TS, Fang WF, Altmann CJ, Douglas IS, Faubel S.** 2008. Interleukin-6 mediates lung injury following ischemic acute kidney injury or bilateral nephrectomy. Kidney Int. **74**:901–909.
51. **Teran LM, Johnston SL, Schroder JM, Church MK, Holgate ST.** 1997. Role of nasal interleukin-8 in neutrophil recruitment and activation in children with virus-induced asthma. Am. J. Respir. Crit. Care Med. **155**:1362–1366.
52. **Jorens PG, Van Damme J, De Backer W, Bossaert L, De Jongh RF, Herman AG, Rampart M.** 1992. Interleukin 8 (IL-8) in the bronchoalveolar lavage fluid from patients with the adult respiratory distress syndrome (ARDS) and patients at risk for ARDS. Cytokine **4**:592–597.
53. **McGuire WW, Spragg RG, Cohen AB, Cochrane CG.** 1982. Studies on the pathogenesis of the adult respiratory distress syndrome. J. Clin. Invest. **69**:543–553.
54. **Rinaldo JE, Borovetz H.** 1985. Deterioration of oxygenation and abnormal lung microvascular permeability during resolution of leukopenia in patients with diffuse lung injury. Am. Rev. Respir. Dis. **131**:579–583.
55. **Weiland JE, Davis WB, Holter JF, Mohammed JR, Dorinsky PM, Gadek JE.** 1986. Lung neutrophils in the adult respiratory distress syndrome. Clinical and pathophysiologic significance. Am. Rev. Respir. Dis. **133**:218–225.
56. **de Jong MD, Simmons CP, Thanh TT, Hien VM, Smith GJ, Chau TN, Hoang DM, Chau NV, Khanh TH, Dong VC, Qui PT, Cam BV, QHa do, Guan Y, Peiris JS, Chinh NT, Hien TT, Farrar J.** 2006. Fatal outcome of human influenza A (H5N1) is associated with high viral load and hypercytokinemia. Nat. Med. **12**:1203–1207.
57. **Wong KT, and Ong KC.** 2011. Pathology of acute henipavirus infection in humans and animals. Pathol. Res. Int. **2011**:567248.
58. **Li M, Embury-Hyatt C, Weingartl HM.** 2010. Experimental inoculation study indicates swine as a potential host for Hendra virus. Vet. Res. **41**:33.
59. **Mathieu C, Guillaume V, Sabine A, Ong KC, Wong KT, Legras-Lachuer C, Horvat B.** 2012. Lethal Nipah virus infection induces rapid overexpression of CXCL10. PLoS One **7**:e32157. doi:10.1371/journal.pone.0032157.
60. **Sousa AR, Lane SJ, Nakhosteen JA, Yoshimura T, Lee TH, Poston RN.** 1994. Increased expression of the monocyte chemoattractant protein-1 in bronchial tissue from asthmatic subjects. Am. J. Respir. Cell Mol. Biol. **10**:142–147.
61. **Asensio VC, Maier J, Milner R, Boztug K, Kincaid C, Moulard M, Phillipson C, Lindsley K, Krucker T, Fox HS, Campbell IL.** 2001. Interferon-independent, human immunodeficiency virus type 1 gp120-mediated induction of CXCL10/IP-10 gene expression by astrocytes in vivo and in vitro. J. Virol. **75**:7067–7077.
62. **Mossman KL, Macgregor PF, Rozmus JJ, Goryachev AB, Edwards AM, Smiley JR.** 2001. Herpes simplex virus triggers and then disarms a host antiviral response. J. Virol. **75**:750–758.
63. **Ruvolo V, Navarro L, Sample CE, David M, Sung S, Swaminathan S.** 2003. The Epstein-Barr virus SM protein induces STAT1 and interferon-stimulated gene expression. J. Virol. **77**:3690–3701.
64. **Basler CF.** 2012. Nipah and Hendra virus interactions with the innate immune system. Curr. Top. Microbiol. Immunol. **359**:123–152.
65. **Ciancanelli MJ, Volchkova VA, Shaw ML, Volchkov VE, Basler CF.** 2009. Nipah virus sequesters inactive STAT1 in the nucleus via a P gene-encoded mechanism. J. Virol. **83**:7828–7841.
66. **Fontana JM, Bankamp B, Rota PA.** 2008. Inhibition of interferon induction and signaling by paramyxoviruses. Immunol. Rev. **225**:46–67.
67. **Park MS, Shaw ML, Munoz-Jordan J, Cros JF, Nakaya T, Bouvier N, Palese P, Garcia-Sastre A, Basler CF.** 2003. Newcastle disease virus (NDV)-based assay demonstrates interferon-antagonist activity for the NDV V protein and the Nipah virus V, W, and C proteins. J. Virol. **77**:1501–1511.
68. **Rodriguez JJ, Parisien JP, Horvath CM.** 2002. Nipah virus V protein evades alpha and gamma interferons by preventing STAT1 and STAT2 activation and nuclear accumulation. J. Virol. **76**:11476–11483.
69. **Shaw ML, Garcia-Sastre A, Palese P, Basler CF.** 2004. Nipah virus V and W proteins have a common STAT1-binding domain yet inhibit STAT1 activation from the cytoplasmic and nuclear compartments, respectively. J. Virol. **78**:5633–5641.
70. **Marsh GA, de Jong C, Barr JA, Tachedjian M, Smith C, Middleton D, Yu M, Todd S, Foord AJ, Haring V, Payne J, Robinson R, Broz I, Crameri G, Field HE, Wang LF.** 2012. Cedar virus: a novel henipavirus isolated from Australian bats. PLoS Pathog. **8**:e1002836. doi:10.1371/journal.ppat.1002836.
71. **Meunier I, von Messling V.** 2011. NS1-mediated delay of type I interferon induction contributes to influenza A virulence in ferrets. J. Gen. Virol. **92**:1635–1644.
72. **Yoneda M, Guillaume V, Sato H, Fujita K, Georges-Courbot MC, Ikeda F, Omi M, Muto-Terao Y, Wild TF, Kai C.** 2010. The nonstructural proteins of Nipah virus play a key role in pathogenicity in experimentally infected animals. PLoS One **5**:e12709. doi:10.1371/journal.pone.0012709.
73. **Psarras S, Volonaki E, Skevaki CL, Xatzipsalti M, Bossios A, Pratsinis H, Tsigkos S, Gourgiotis D, Constantopoulos AG, Papapetropoulos A, Saxoni-Papageorgiou P, Papadopoulos NG.** 2006. Vascular endothelial growth factor-mediated induction of angiogenesis by human rhinoviruses. J. Allergy Clin. Immunol. **117**:291–297.
74. **Yancopoulos GD, Davis S, Gale NW, Rudge JS, Wiegand SJ, Holash J.** 2000. Vascular-specific growth factors and blood vessel formation. Nature **407**:242–248.